

Massive MIMO Channel Estimation with Low-Resolution Spatial Sigma-Delta ADCs

Shilpa Rao¹, Gonzalo Seco-Granados², Hessam Pirzadeh¹, and A. Lee Swindlehurst¹

¹Center for Pervasive Communications and Computing, University of California, Irvine

²Department of Telecommunications and Systems Engineering, Universitat Autònoma de Barcelona

Abstract—We consider channel estimation for an uplink massive multiple input multiple output (MIMO) system where the base station (BS) uses an array with low-resolution (1-2 bit) analog-to-digital converters and a spatial Sigma-Delta ($\Sigma\Delta$) architecture to shape the quantization noise away from users in some angular sector. We develop a linear minimum mean squared error (LMMSE) channel estimator based on the Bussgang decomposition that reformulates the nonlinear quantizer model using an equivalent linear model plus quantization noise. We also analyze the uplink achievable rate with maximal ratio combining (MRC) and zero-forcing (ZF) receivers and provide a closed-form expression for the achievable rate with the MRC receiver. Numerical results show superior channel estimation and sum spectral efficiency performance using the $\Sigma\Delta$ architecture compared to conventional 1- or 2-bit quantized massive MIMO systems.

I. INTRODUCTION

Massive MIMO systems provide high spatial resolution and throughput, but the cost and power consumption of the associated RF hardware, particularly the analog-to-digital converters (ADCs) and digital-to-analog converters (DACs) can be prohibitive, especially at higher bandwidths and sampling rates. To save power and chip area, low-resolution quantizers have been suggested. The simple design and low power consumption of low-resolution ADCs/DACs have made them very suitable for massive MIMO.

There has been extensive research on one-bit ADCs, in particular, for uplink transmission [1–6] and downlink precoding [7–12]. Channel estimation with GAMP [13], near ML [4] and linear estimators [1], [14] using one-bit ADCs, MMSE channel estimation based on recursive least-squares using two-bit ADCs [15] and with dithered feedback signals [16] using 1-3 bit ADCs have been proposed. In addition to savings in energy and circuit complexity, one-bit ADCs also reduce the fronthaul throughput from the remote radio head (RRH) in cellular applications. This is a significant issue for massive MIMO implementations operating with high bandwidths, as in a millimeter wave application; a 100-element antenna array sampled at 500 Msamples/sec with a 10-bit ADC requires a 1 Tb/sec data pipeline from the RRH to the baseband processor. One-bit sampling can significantly alleviate this requirement. While it has been shown that one-bit quantization causes only

a small degradation at low SNRs and offers significant advantages in terms of power consumption and implementation complexity, at medium to high SNRs the performance loss is substantial.

One method to improve the performance is to simply increase the number of quantization bits. Simulations have shown that using ADCs with 3-5 bits of resolution in massive MIMO provides performance that is very close to that achievable with infinite precision, and achieves a good trade-off between energy and spectral efficiency [17], [18]. Alternatively, the sampling rate at which the one-bit quantizers operate can also be increased, and this approach has been studied in [19–21]. A well-known technique that combines one-bit quantization and oversampling is the $\Sigma\Delta$ ADC, which to date has primarily found application in ultrasound imaging, automotive radar and pulse-coded modulation for audio encoding. The temporal $\Sigma\Delta$ converter scheme consists of an oversampled modulator, responsible for digitization of the analog signal, followed by a negative feedback loop that shapes the quantization noise with a simple high-pass filter. The quantization noise can then be removed in favor of the desired signal using a digital lowpass filter and decimation (if necessary). The temporal $\Sigma\Delta$ architecture has been extensively studied over the years [22–25], and higher-order implementations exist that can provide additional frequency-selective noise shaping. The use of $\Sigma\Delta$ ADCs in parallel architectures for MIMO systems has been studied in [26], [27]. While higher-resolution ADCs and temporal oversampling can improve performance with only a moderate increase in power consumption, they significantly increase the required fronthaul throughput compared with one-bit quantization.

A noise-shaping effect analogous to that achieved by temporal $\Sigma\Delta$ quantizers can be achieved by implementing the $\Sigma\Delta$ architecture in the spatial domain. This approach exploits oversampling in space, which can occur in massive MIMO settings with a limited array aperture, or for scenarios where the uplink signals are confined to a given angular sector, due to cell sectorization, limited multipath scattering (e.g., as at millimeter wave frequencies), or certain small-cell geometries (narrow conference halls, city streets, etc.). In a system employing spatial $\Sigma\Delta$ ADCs, the quantization error from the ADC at one antenna is fed to the input of an adjacent antenna, rather than to the input of the same antenna. In a standard implementation without phase-shifting the feedback, this has the effect of shaping the quantization noise to high spatial

frequencies, in favor of user signals that arrive from angles closer to the broadside of the array, which correspond to low spatial frequencies. While spatial oversampling, i.e., antennas spaced less than one-half wavelength apart, can produce the required low spatial frequencies for the user signals, there is a limit to how close the antennas can be placed together before mutual coupling and the physical size of the antennas come into play. For this reason, a more likely scenario is that some small degree of spatial oversampling would be combined with the assumption that the users of interest are already confined to some angular sector, since one can easily steer the angular sector of low quantization noise to arbitrary directions.

While temporal $\Sigma\Delta$ systems have been studied for decades, there is relatively little work on corresponding spatial implementations. Only recently has the noise shaping characteristics of first and second-order spatial and cascaded space-time $\Sigma\Delta$ architectures been studied for a few array processing applications. In particular, applications have been considered for massive MIMO [28–32], phased arrays [33], [34], interference cancellation [27], and spatio-temporal $\Sigma\Delta$ circuit implementations [35], [36]. With the exception of our preliminary study in [30], there has been no prior work focused on channel estimation for spatial $\Sigma\Delta$ massive MIMO systems.

In this paper, we consider optimal linear minimum mean squared error (LMMSE) channel estimation for massive MIMO systems with first-order one-bit and two-bit spatial $\Sigma\Delta$ ADCs. Our initial results on this problem in [30] were derived based on a vector-wise Bussgang decomposition similar to what was used for standard one-bit quantization in [1]. However, this approach leads to a mathematical model in which the quantization error vector is defined to be uncorrelated with the input vector to the $\Sigma\Delta$ quantizer, which is not consistent with the more traditional definition of quantization noise based on the actual system architecture. Based on this observation, we have modified our analysis to incorporate a more meaningful definition of the quantization noise, using an element-wise implementation of the Bussgang decomposition as defined in [32] in order to find an equivalent linear signal-plus-quantization-noise representation. Our approach also explicitly takes into account the spatial correlation between the quantized outputs of the $\Sigma\Delta$ ADC array.

The structure of the $\Sigma\Delta$ array allows us to find a recursive solution for the covariance matrices required to compute the LMMSE channel estimate, and also to derive analytical expressions for the resulting normalized mean squared error (NMSE). After performing the analysis for the one-bit case, we show how the LMMSE channel estimate and analytical NMSE performance characterization can be extended for a $\Sigma\Delta$ array implemented with two-bit quantization. The resulting estimators in both cases have low complexity and the simulated estimation error closely matches the derived analytical expressions. Our simulation results indicate that, at low-to-medium SNRs, the LMMSE channel estimator for the $\Sigma\Delta$ array yields channel estimates that are very close to those achieved with infinite resolution ADCs. The inevitable error floor at high SNR is significantly lower than that achieved by standard one-bit and two-bit quantization; for example, the one-bit $\Sigma\Delta$ LMMSE channel estimate has an NMSE that is

two orders of magnitude smaller than that achieved by standard two-bit quantization.

The spectral efficiency of one-bit $\Sigma\Delta$ arrays was recently analyzed in [32], but only for the case where the channel is known. In this paper, we also extend the analysis of [32] to derive a lower bound on the uplink achievable rate using maximal ratio combining (MRC) and zero-forcing (ZF) receivers when implemented with imperfect channel state information (CSI) based on our LMMSE channel estimate. We derive a closed-form expression for the spectral efficiency of MRC, while for the ZF receiver we present simulated results. In both cases, the results of our spectral efficiency analysis show that the $\Sigma\Delta$ architecture significantly outperforms standard low-resolution (1-2 bits) quantization. For a ZF receiver, the $\Sigma\Delta$ implementation achieves three times the spectral efficiency of standard one- and two-bit approaches. For the case of MRC, the two-bit $\Sigma\Delta$ architecture provides 99% of the spectral efficiency of system with infinite resolution ADCs.

The rest of the paper is organized as follows. In Section II, we describe the assumed signal and channel model, and then in Section III we present the first-order spatial $\Sigma\Delta$ array architecture. Section IV derives the corresponding linear Bussgang model that describes the input-output relationship of the spatial $\Sigma\Delta$ array. LMMSE channel estimators based on the output of the one-bit or two-bit spatial $\Sigma\Delta$ ADC array are then derived in Section V, and the bounds on the uplink achievable rate are calculated in Section VI. Simulation results validating our analyses are presented in Section VII.

Notation: Boldface lowercase variables denote vectors and boldface uppercase variables denote matrices. \mathbf{X}^T , \mathbf{X}^H and \mathbf{X}^* are the transpose, Hermitian transpose, and conjugate of \mathbf{X} , respectively. The i th element of vector \mathbf{x} is represented by x_i . The symbols \otimes and $\text{vec}(\cdot)$ respectively represent the Kronecker product and the vectorization operation, i.e., the stacking of the columns of a matrix one below the other. Real and imaginary parts are indicated by $\text{Re}(\cdot)$ and $\text{Im}(\cdot)$, respectively. $\mathbb{E}(\cdot)$ is the expectation operator. $\text{Tr}(\mathbf{X})$ is the trace of the matrix \mathbf{X} and \mathbf{X}^\dagger denotes pseudo-inverse of \mathbf{X} . The matrix \mathbf{I}_p denotes a $p \times p$ identity matrix. The function $\text{mod}_M(\cdot)$ represents the modulo- M operator, and $\lfloor z \rfloor$ is the largest integer smaller than z . A circularly symmetric complex Gaussian vector with mean \mathbf{a} and covariance matrix \mathbf{B} is denoted by $\mathbf{x} \sim \mathcal{CN}(\mathbf{a}, \mathbf{B})$. The cumulative distribution function (cdf) and the standard normal density are given by $\Psi(x)$ and $\Psi'(x)$, respectively.

II. SYSTEM MODEL

We consider an uplink massive MIMO system with K single-antenna user terminals, and a base station (BS) equipped with a uniform linear array (ULA) of M antennas and a first-order spatial $\Sigma\Delta$ array. During the training period, all K users transmit their pilot sequences of length N simultaneously. The received signal, $\mathbf{X} \in \mathbb{C}^{M \times N}$, at the BS is

$$\mathbf{X} = [\mathbf{x}_1 \cdots \mathbf{x}_N] = \sqrt{\rho} \mathbf{G} \Phi_t + \mathbf{N}, \quad (1)$$

where we assume that all the user signals are received with the same power and, therefore, ρ is a factor that determines the

SNR, \mathbf{x}_k is the array output for training sample k , $\mathbf{G} \in \mathbb{C}^{M \times K}$ is the channel matrix, $\Phi_t \in \mathbb{C}^{K \times N}$ is the pilot matrix and \mathbf{N} contains additive noise with independent and identically distributed (i.i.d.) Gaussian elements: $[\mathbf{N}]_{ij} \sim \mathcal{CN}(0, 1)$.

We consider a channel that is composed of L paths for each user with a certain angular spread Θ . More specifically, the k th column of \mathbf{G} represents the channel \mathbf{g}_k for the k th user, and is given by

$$\mathbf{g}_k = \frac{1}{\sqrt{L}} \mathbf{A} \mathbf{h}_k, \quad (2)$$

where the elements of \mathbf{h}_k are independently and identically distributed (i.i.d.) as $\mathcal{CN}(0, 1)$ random variables, and $\mathbf{A} \in \mathbb{C}^{M \times L}$ is a matrix whose l th column is the steering vector

$$\mathbf{a}_l = \left[1 \ e^{-j2\pi\delta\sin(\theta_l)} \ \dots \ e^{-j2\pi\delta(M-1)\sin(\theta_l)} \right]^T, \quad (3)$$

where $\delta = d/\lambda$ is the inter-element antenna spacing in terms of the wavelength and $\theta_l \in \left[-\frac{\Theta}{2}, \frac{\Theta}{2}\right]$. Thus, the channel \mathbf{G} is given by $\mathbf{G} = \frac{1}{\sqrt{L}} \mathbf{A} \mathbf{H}$, where $\mathbf{H} = [\mathbf{h}_1, \mathbf{h}_2, \dots, \mathbf{h}_K]$, and the channel covariance matrix is given by $\mathbf{C}_G = \frac{1}{L} \mathbf{A} \mathbf{A}^H$, which we assume to be known. This is equivalent to knowing *a priori* the sector over which the users are distributed; the matrix \mathbf{A} can be populated by steering vectors uniformly spaced across the sector.

Vectorizing (1) and letting $\Phi = \sqrt{\rho} (\Phi_t^T \otimes \mathbf{I}_M)$, $\mathbf{g} = \text{vec}(\mathbf{G})$ and $\mathbf{n} = \text{vec}(\mathbf{N})$, we get

$$\mathbf{x} = \text{vec}(\mathbf{X}) = \Phi \mathbf{g} + \mathbf{n}. \quad (4)$$

The covariance matrix of \mathbf{x} can be expressed as

$$\mathbf{C}_x = \Phi \mathbf{C}_g \Phi^H + \mathbf{I}_{MN}, \quad (5)$$

where $\mathbf{C}_g = \mathbf{I}_K \otimes \mathbf{C}_G$ is block-diagonal. The SNR per-user per-antenna is

$$\text{SNR} = \frac{\rho}{MK} \text{Tr} \left(\mathbb{E} \left[\mathbf{G} \Phi_t \Phi_t^H \mathbf{G}^H \right] \right). \quad (6)$$

When the pilot sequences are row-wise orthogonal and the minimum number of pilots, $N = K$, is used, then $\Phi_t \Phi_t^H = K \mathbf{I}_K$ and the SNR is equal to ρ . In the derivations below, we will assume that the power of the pilot signals is time-invariant, which implies that the diagonal elements of $\Phi_t^H \Phi_t$ are identical.

III. FIRST-ORDER SPATIAL $\Sigma\Delta$ ARCHITECTURE

A first-order temporal $\Sigma\Delta$ modulator can be described by the block diagram depicted in Fig. 1a. The architecture consists of a low-resolution quantizer $\mathcal{Q}(\cdot)$ and a negative feedback loop where the difference between the output and input of the quantizer is subtracted from the antenna input $x[n]$ after a one-sample delay. The operation of the quantizer is defined using the following equivalent linear model with gain $\gamma > 0$:

$$y[n] = \mathcal{Q}(r[n]) = \gamma r[n] + q[n]. \quad (7)$$

While the gain of the quantizer is normally taken to be simply $\gamma = 1$, we consider this more general case since it is relevant

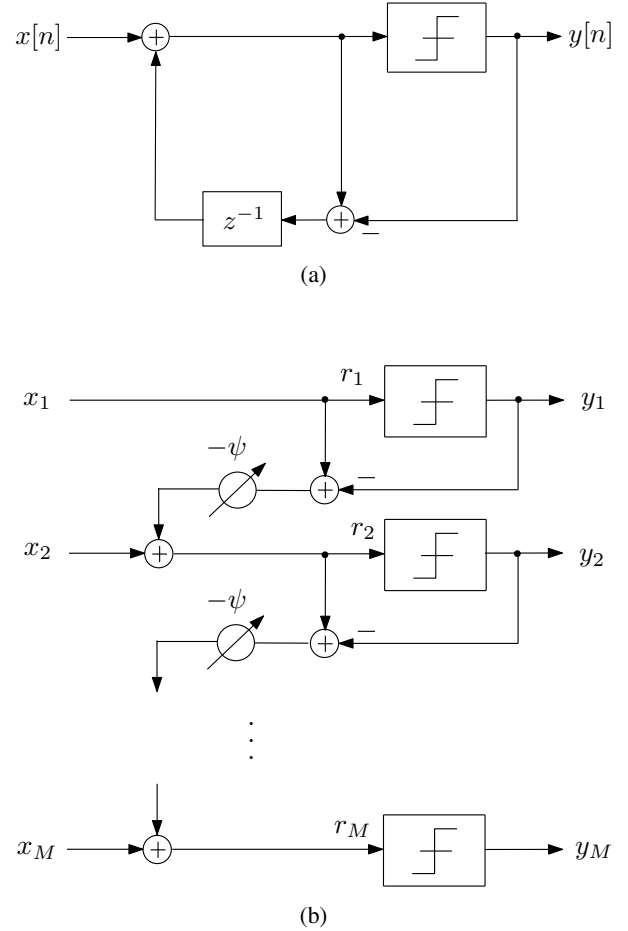


Fig. 1: (a) A first-order temporal $\Sigma\Delta$ modulator. (b) A first-order one-bit $\Sigma\Delta$ array steered to direction ψ .

to our subsequent analysis. As shown in [32], this leads to the following transfer function description of the $\Sigma\Delta$ modulator:

$$\begin{aligned} Y(z) &= \frac{\gamma}{1 - (\gamma - 1)z^{-1}} X(z) + \frac{(1 - z^{-1})}{1 - (\gamma - 1)z^{-1}} Q(z) \\ &= A_x(z) X(z) + A_q(z) Q(z), \end{aligned}$$

where $\{Y(z), X(z), Q(z)\}$ respectively represent the z -transforms of $\{y[n], x[n], q[n]\}$. When $\gamma = 1$, we have that $A_x(z) = 1$ is an all-pass filter and that $A_q(z) = 1 - z^{-1}$ is a first-order high-pass filter, which is the standard result, indicating the quantization noise is shaped to higher frequencies. Given that $x[n]$ is oversampled and is concentrated at lower frequencies, the effect of the quantization noise can be substantially reduced by passing the output of the $\Sigma\Delta$ modulator through a low-pass filter. The all-pass plus high-pass structure still remains true as long as $\gamma \approx 1$, but the $\Sigma\Delta$ modulator approaches instability as $\gamma \rightarrow 2$.

Quantization noise shaping can also be achieved in the spatial domain by propagating the quantization error from one antenna to the next, in effect exploiting spatial rather than temporal correlation in the desired signal. The spatial $\Sigma\Delta$ architecture is depicted in Fig. 1b, and shows that the quantization error from one antenna is phase-shifted by $-\phi$ prior to being added to the input of the adjacent antenna. This

architecture shapes the quantization noise away from the angle of arrival (AoA) associated with the phase shift ϕ , and thus users in an angular sector surrounding this AoA experience a significantly higher signal-to-quantization-noise ratio (SQNR). The size of the high-SQNR angular sector can be increased by placing the antennas closer together than $\lambda/2$, corresponding to spatial oversampling, although in practice mutual coupling and the physical dimensions of the antennas place a limit on how much spatial oversampling can be achieved.

To generate a mathematical model for the $\Sigma\Delta$ array, define the $MN \times 1$ vectors \mathbf{r} and \mathbf{y} corresponding respectively to the quantizer inputs and the array outputs that result from the $MN \times 1$ received signal vector \mathbf{x} in (4). In other words, the m th elements $\{x_m, r_m, y_m\}$ of the vectors $\{\mathbf{x}, \mathbf{r}, \mathbf{y}\}$ respectively represent the signal received by antenna $\text{mod}_M(m)$, the input to the quantizer at antenna $\text{mod}_M(m)$, and the $\Sigma\Delta$ output of antenna $\text{mod}_M(m)$ for training sample $\lfloor \frac{m}{M} \rfloor$. Defining $m' = \text{mod}_M(m)$, we thus have

$$y_m = \alpha_{rm'} \mathcal{Q}_{m'}(\text{Re}(r_m)) + j\alpha_{im'} \mathcal{Q}_{m'}(\text{Im}(r_m)), \quad (8)$$

where $\mathcal{Q}_{m'}$ represents the quantization operation for antenna m' , and $\alpha_{rm'}$ and $\alpha_{im'}$ are the output levels for the real and imaginary parts of the quantizer, respectively. Note that we assume the output level of the quantizer in general to be different for each antenna, unlike conventional one-bit quantization where the output levels for all the antennas are the same. In vector form, the output of the $\Sigma\Delta$ array can be written as

$$\mathbf{y} = \mathcal{Q}(\mathbf{r}) = [\mathcal{Q}_1(r_1), \dots, \mathcal{Q}_M(r_M), \mathcal{Q}_1(r_{M+1}), \dots, \mathcal{Q}_M(r_{MN})]^T, \quad (9)$$

where

$$\mathbf{r} = \mathbf{U}\mathbf{x} - \mathbf{V}\mathbf{y},$$

$$\mathbf{V} = \mathbf{I}_N \otimes \underbrace{\begin{bmatrix} 0 & 0 & \dots & 0 & 0 \\ e^{-j\psi} & 0 & \dots & 0 & 0 \\ e^{-j2\psi} & e^{-j\psi} & \dots & 0 & 0 \\ \vdots & \vdots & \ddots & \vdots & \vdots \\ e^{-j(M-1)\psi} & e^{-j(M-2)\psi} & \dots & e^{-j\psi} & 0 \end{bmatrix}}_{\mathbf{V}_d},$$

$$\mathbf{U} = \mathbf{I}_N \otimes \underbrace{(\mathbf{I}_M + \mathbf{V}_d)}_{\mathbf{U}_d}. \quad (10)$$

IV. EQUIVALENT LINEAR MODEL FOR THE SPATIAL $\Sigma\Delta$ ARRAY

As in the scalar case described by (7), we will represent the operation of the $\Sigma\Delta$ array using an equivalent linear model defined by

$$\mathbf{y} = \mathbf{\Gamma}\mathbf{r} + \mathbf{q} \quad (11)$$

for a given matrix $\mathbf{\Gamma}$, where \mathbf{q} is the equivalent quantization noise. There are an infinite number of such models, one for every choice of $\mathbf{\Gamma}$, and each will result in a particular definition for the quantization noise with differing statistical properties. One possible choice for the matrix $\mathbf{\Gamma}$ is obtained by making \mathbf{r} uncorrelated with \mathbf{q} , i.e. $\mathbb{E}[\mathbf{r}\mathbf{q}^H] = 0$. This leads to

$\mathbf{\Gamma} = \mathbf{C}_{yr}\mathbf{C}_r^{-1}$, where $\mathbf{C}_{yr} = \mathbb{E}[\mathbf{y}\mathbf{r}^H]$ is the cross-covariance matrix between \mathbf{y} and \mathbf{r} , and \mathbf{C}_r is the covariance matrix of \mathbf{r} . Assuming the elements of \mathbf{r} are jointly Gaussian, the Bussgang theorem can be applied. This approach was used to derive channel estimates in [1] for conventional one-bit quantization, and in our initial work on the $\Sigma\Delta$ array [30]. However, the resulting definition for the quantization noise does not have a physical interpretation in the context of Fig. 1b.

Instead, we define $\mathbf{\Gamma}$ following the approach of [32], again assuming that \mathbf{r} is Gaussian, but applying the Bussgang decomposition element-wise such that $\mathbb{E}[r_m q_m^*] = 0$. Further assuming that the elements of \mathbf{r} are circularly symmetric, the quantizer output levels $\alpha_{rm'}$ and $\alpha_{im'}$ are identical, and we can set $\alpha_{rm'} = \alpha_{im'} = \alpha_{m'}$. With this definition, $\mathbf{\Gamma}$ becomes a diagonal matrix whose m th diagonal element, γ_m , is given by

$$\gamma_m = \frac{\mathbb{E}(r_m y_m^*)}{\mathbb{E}(|r_m|^2)}. \quad (12)$$

Plugging $\mathbf{r} = \mathbf{U}\mathbf{x} - \mathbf{V}\mathbf{y}$ into (11), we get

$$\mathbf{y} = (\mathbf{I} + \mathbf{\Gamma}\mathbf{V})^{-1} \mathbf{\Gamma}\mathbf{U}\mathbf{x} + (\mathbf{I} + \mathbf{\Gamma}\mathbf{V})^{-1} \mathbf{q}. \quad (13)$$

The specific numerical value for γ_m will depend on the output level $\alpha_{m'}$. Assuming that the statistics of the received data are time-invariant over the current channel coherence interval, we can choose $\alpha_{m'}$ such that $\gamma_m = 1$, or equivalently such that $\mathbf{\Gamma} = \mathbf{I}_{MN}$, and (13) can be simplified to

$$\mathbf{y} = \mathbf{x} + \mathbf{U}^{-1}\mathbf{q}. \quad (14)$$

This model is now the exact spatial analog of the temporal $\Sigma\Delta$ architecture, and is equivalent to passing \mathbf{x} through a (spatial) all-pass filter and \mathbf{q} through a filter that shapes the quantization noise away from the AoA corresponding to ψ . In the discussion that follows, we will derive expressions for the values of $\alpha_{m'}$ necessary to achieve $\gamma_m = 1$ for the case of one-bit and two-bit quantization, as well as the resulting power of the quantization noise on each antenna. The resulting expressions for $\alpha_{m'}$ will depend in general on the power of the signal r_m , which would have to remain time-invariant for the quantizer gains to be fixed. This can be achieved in practice using an automatic gain control at the input to the ADC.

A. One-Bit Spatial $\Sigma\Delta$ ADCs

When the $\Sigma\Delta$ array is implemented with one-bit ADCs, the output is given by

$$y_m = \alpha_{m'} (\text{sign}(\text{Re}(r_m)) + j\text{sign}(\text{Im}(r_m))), \quad (15)$$

and (12) can be simplified to get

$$\begin{aligned} \gamma_m &= \alpha_{m'} \frac{\mathbb{E}(|\text{Re}(r_m)| + |\text{Im}(r_m)|)}{\mathbb{E}(|r_m|^2)} \\ &= \alpha_{m'} \frac{\mathbb{E}(|\text{Re}(r_m)|)}{\mathbb{E}(|\text{Re}(r_m)|^2)} \end{aligned} \quad (16)$$

for circularly symmetric r_m . Assuming that the power of the pilot symbols is time-invariant, then the statistics of r_m are identical to those of $r_{m'}$. Consequently, we can set $\gamma_m = 1$, which leads to

$$\alpha_{m'} = \frac{\mathbb{E}(|\text{Re}(r_m)|^2)}{\mathbb{E}(|\text{Re}(r_m)|)}.$$

To simplify the expression, in [32] it was assumed that r_m is Gaussian, in which case

$$\alpha_{m'} = \frac{\sqrt{\pi \mathbb{E}(|r_m|^2)}}{2}. \quad (17)$$

The derivation of (17) relies on the fact that

$$\frac{\sqrt{\mathbb{E}(|\operatorname{Re}(r_m)|^2)}}{\mathbb{E}(|\operatorname{Re}(r_m)|)} = \sqrt{\frac{\pi}{2}} \quad (18)$$

for Gaussian random variables. However, due to the non-linear feedback structure of the $\Sigma\Delta$ array, the tails of the distribution of r_m are slightly heavier than a Gaussian, so the ratio on the left hand side of (18) is slightly greater than $\sqrt{\pi/2}$. For this reason, we will choose a slightly larger value for $\alpha_{m'}$ than in (17):

$$\alpha_{m'}^* = \beta \frac{\sqrt{\pi \mathbb{E}(|r_m|^2)}}{2}, \quad (19)$$

where $\beta > 1$ is a correction factor. This is consistent with prior work on temporal $\Sigma\Delta$ quantization, which has shown that slightly increasing the power of the input signal $x[n]$ for fixed output levels (or equivalently, decreasing the output levels for fixed input signal power) reduces the quantization noise [25], [37], [38]. This benefit is lost if one applies too large an increase in the input power, as the input to the quantizer quickly becomes unstable. In fact, as we show below, for the $\Sigma\Delta$ array there is a very small range of values near one that are appropriate for the correction factor β . While we could set $\beta = 1$ as in [32], better channel estimation results and a better match with the analytical expressions are obtained when a value slightly larger than one is used, especially when the array input has high spatial correlation due to spatial oversampling (i.e., small δ) or a small angular spread.

Let $\sigma_{r_m}^2 \triangleq \mathbb{E}(|r_m|^2)$. Using similar definitions for $\sigma_{y_m}^2$ and $\sigma_{q_m}^2$, and the fact that r_m and q_m are uncorrelated, we obtain the following relationship between the powers of the input and output of the array:

$$\sigma_{y_m}^2 = \frac{\pi}{2} \beta^2 \sigma_{r_m}^2, \quad \sigma_{q_m}^2 = \sigma_{y_m}^2 - \sigma_{r_m}^2. \quad (20)$$

From (20), we can see that in order to prevent the quantization noise power from becoming greater than the input power $\sigma_{r_m}^2$, we must ensure that $(\frac{\pi}{2} \beta^2 - 1) < 1$, and hence that $1 \leq \beta < 2/\sqrt{\pi} \approx 1.1284$. Otherwise, the input power to each ADC grows monotonically with the antenna index, as will become apparent in the channel estimation recursion derived in Section V-A. We have found that the performance of the one-bit $\Sigma\Delta$ quantizer begins to degrade for values of β close to the extremes of the interval $1 \leq \beta \leq 2/\sqrt{\pi}$, and that good performance can be achieved using a value near the midpoint, e.g., $\beta \approx 1.05$.

B. Two-bit Spatial $\Sigma\Delta$ ADCs

In this section, we extend the above analysis to the case where the quantizers in the $\Sigma\Delta$ array employ two-bits of resolution, implying four quantization levels. We use the well-known Lloyd-max condition to determine the optimum quantization levels that minimize the distortion [39], [40]. We will denote the quantization levels and the associated intervals

that minimize the distortion for unit variance Gaussian inputs by ν_i and $(\nu_i^{\text{lo}}, \nu_i^{\text{hi}})$, $i = 1, \dots, 4$, respectively. That is, for a generic Gaussian random variable with unit variance, x ,

$$\mathcal{Q}(x) = \nu_i, \quad \text{if } x \in (\nu_i^{\text{lo}}, \nu_i^{\text{hi}}]. \quad (21)$$

The quantization levels satisfy $\nu_i^{\text{hi}} = \nu_{i+1}^{\text{lo}}$, $\nu_1^{\text{lo}} = -\infty$, and $\nu_4^{\text{hi}} = \infty$. Since we assume that the input to the m th $\Sigma\Delta$ ADC is a circularly symmetric Gaussian random variable with variance $\sigma_{r_m}^2$, the quantization bins should be adjusted to span the range of the input levels. Denoting $\operatorname{Re}(r_m)$ by r_m^{Re} ,

$$\mathcal{Q}_{m'}(r_m^{\text{Re}}) = \frac{\sigma_{r_m}}{\sqrt{2}} \nu_i, \quad \text{if } r_m^{\text{Re}} \in \left(\frac{\sigma_{r_m}}{\sqrt{2}} \nu_i^{\text{lo}}, \frac{\sigma_{r_m}}{\sqrt{2}} \nu_i^{\text{hi}} \right], \quad (22)$$

and

$$y_m = \alpha_{m'} (\mathcal{Q}_{m'}(\operatorname{Re}(r_m)) + j \mathcal{Q}_{m'}(\operatorname{Im}(r_m))), \quad (23)$$

where as before the factor $\alpha_{m'}$ is the same for both the real and imaginary parts since r_m is assumed to be circularly symmetric.

Assuming a linear model as before and using an element-wise Bussgang decomposition, due to the circular symmetry of the data, Eq. (12) can be written as

$$\gamma_m = \frac{\mathbb{E}[r_m^{\text{Re}} y_m^{\text{Re}}]}{\mathbb{E}[r_m^{\text{Re}}]^2}, \quad (24)$$

where $y_m^{\text{Re}} \triangleq \operatorname{Re}(y_m)$ and $\mathbb{E}[r_m^{\text{Re}} y_m^{\text{Re}}]$ is obtained from Price's theorem [41] and is a function of the quantization levels and the decision thresholds. The theorem states that the correlation between the input and the output has the following derivative

$$\begin{aligned} & \frac{\partial \mathbb{E}[r_m^{\text{Re}} \mathcal{Q}_{m'}(r_m^{\text{Re}})]}{\partial r_m^{\text{Re}}} \\ &= \frac{\sigma_{r_m}}{\sqrt{2}} \int_{-\infty}^{\infty} \frac{1}{\sqrt{2\pi}} \frac{\partial \mathcal{Q}_{m'}(r_m^{\text{Re}})}{\partial r_m^{\text{Re}}} \exp\left(-\frac{(r_m^{\text{Re}})^2}{\sigma_{r_m}^2}\right) dr_m^{\text{Re}}. \end{aligned} \quad (25)$$

The derivative $\partial \mathcal{Q}_{m'}(r_m^{\text{Re}}) / \partial r_m^{\text{Re}}$ can be computed as

$$\frac{\partial \mathcal{Q}_{m'}(r_m^{\text{Re}})}{\partial r_m^{\text{Re}}} = \frac{\sigma_{r_m}}{\sqrt{2}} \sum_{i=2}^4 (\nu_i - \nu_{i-1}) \delta\left(r_m^{\text{Re}} - \frac{\sigma_{r_m}}{\sqrt{2}} \nu_i^{\text{lo}}\right). \quad (26)$$

Substituting the above equation in (25) and evaluating the integral, we get

$$\mathbb{E}[r_m^{\text{Re}} y_m^{\text{Re}}] = \alpha_{m'} \frac{\sigma_{r_m}^2}{2} \sum_{i=2}^4 \frac{(\nu_i - \nu_{i-1})}{\sqrt{2\pi}} \exp\left(-\frac{(\nu_i^{\text{lo}})^2}{2}\right). \quad (27)$$

Then, the value of $\alpha_{m'}$ that yields $\gamma_m = 1$ is given by

$$\alpha_{m'} = \frac{\sqrt{2\pi}}{\sum_{i=2}^4 (\nu_i - \nu_{i-1}) \exp\left(-\frac{(\nu_i^{\text{lo}})^2}{2}\right)}. \quad (28)$$

From (28), we can see that, unlike the one-bit case, $\alpha_{m'}$ is not dependent on the index m' at all for the $\Sigma\Delta$ array with two-bit quantization. Instead, it is a constant determined only by the quantization intervals and the corresponding levels. This is because the quantization levels and the intervals for the m' th ADC have been scaled by the standard deviation of the input.

Therefore, $\alpha_{m'}$ corresponds to an additional correction that has to be applied to make $\gamma_m = 1$. In the remainder of this discussion, we will drop the dependence on m' and use α to denote $\alpha_{m'}$. Finally, computing the expectation $\mathbb{E}[\|y_m\|^2]$, the output and quantization noise powers are, respectively, given by

$$\begin{aligned}\sigma_{y_m}^2 &= \alpha^2 \sum_i |\mathcal{Q}_{m'}(r_m^{\text{Re}})|^2 \Pr\left(\frac{\sigma_{r_m}}{\sqrt{2}} \nu_i^{\text{lo}} < r_m^{\text{Re}} \leq \frac{\sigma_{r_m}}{\sqrt{2}} \nu_i^{\text{hi}}\right) \\ &= \frac{\alpha^2 \sigma_{r_m}^2}{2} \sum_{i=1}^4 \nu_i^2 \left(\Psi\left(\frac{\sigma_{r_m}}{\sqrt{2}} \nu_i^{\text{hi}}\right) - \Psi\left(\frac{\sigma_{r_m}}{\sqrt{2}} \nu_i^{\text{lo}}\right) \right), \\ \sigma_{q_m}^2 &= \sigma_{y_m}^2 - \sigma_{r_m}^2,\end{aligned}\quad (29)$$

where $\Psi(\cdot)$ is the cumulative distribution function of the normal distribution.

One distinction between the one- and two-bit $\Sigma\Delta$ operation is the correction factor β . Unlike the one-bit case, the two-bit $\Sigma\Delta$ ADC shows little dependence on β since increasing the number of bits results in a quantization error that is more accurately characterized as Gaussian. As a result, we omit this correction factor altogether for the two-bit case and still achieve good performance.

V. CHANNEL ESTIMATION WITH SPATIAL $\Sigma\Delta$ ADCs

By describing the input-output relationship with an equivalent linear model, we were able to arrive at closed-form expressions for the quantization noise and output powers in Eqs. (20) and (29). Leveraging the results derived in the previous section, we derive below the LMMSE channel estimate based on the one-bit or two-bit outputs of the $\Sigma\Delta$ ADC array, \mathbf{y} .

A. LMMSE Channel Estimation

The LMMSE channel estimate is defined by

$$\begin{aligned}\hat{\mathbf{g}} &= \mathbb{E}[\mathbf{g}\mathbf{y}^H] (\mathbb{E}[\mathbf{y}\mathbf{y}^H])^{-1} \mathbf{y} \\ &= \mathbf{C}_{gy} \mathbf{C}_y^{-1} \mathbf{y}.\end{aligned}\quad (30)$$

In Appendix A, we show that $\mathbb{E}[\mathbf{x}\mathbf{q}^H] \approx \mathbf{0}$, and hence from (14), we can obtain the covariance matrix of \mathbf{y} :

$$\mathbf{C}_y = \mathbf{C}_x + \mathbf{U}^{-1} \mathbf{C}_q \mathbf{U}^{-H}, \quad (31)$$

where \mathbf{C}_q is the covariance matrix of \mathbf{q} . Similarly, since we have chosen $\mathbf{\Gamma} = \mathbf{I}$ in (11), it is easy to show that

$$\mathbf{r} = \mathbf{x} - \mathbf{U}^{-1} \mathbf{V} \mathbf{q} \quad (32)$$

and hence that

$$\mathbf{C}_r = \mathbf{C}_x + \mathbf{U}^{-1} \mathbf{V} \mathbf{C}_q \mathbf{V}^H \mathbf{U}^{-H}. \quad (33)$$

From (31), we see that \mathbf{C}_y is determined by \mathbf{C}_q , whereas (20) and (29) show that the quantization noise power is dependent on $\sigma_{y_m}^2$. Due to this inter-relationship between \mathbf{C}_y and \mathbf{C}_q , these matrices cannot be computed in closed form. However, they can be computed in a recursive manner.

Using $\mathbb{E}[\mathbf{x}\mathbf{q}^H] \approx \mathbf{0}$ and the fact that $\mathbb{E}[r_m q_m^*] = 0$, we can show that $\mathbb{E}[q_m q_{m\pm 1}^*] \approx 0$. As a result, \mathbf{C}_q is approximately

diagonal with elements given by $\sigma_{q_m}^2$. Furthermore, noting that $\mathbf{U}^{-1} \mathbf{V}$ has the structure

$$\mathbf{U}^{-1} \mathbf{V} = \mathbf{I}_N \otimes e^{-j\psi} \begin{bmatrix} 0 & 0 & \dots & 0 & 0 \\ 1 & 0 & \dots & 0 & 0 \\ 0 & 1 & \dots & 0 & 0 \\ & & \vdots & & \\ 0 & 0 & \dots & 1 & 0 \end{bmatrix}, \quad (34)$$

we can generate the following recursion for $\sigma_{r_m}^2$, $\sigma_{y_m}^2$ and $\sigma_{q_m}^2$ using Eqs. (31) and (33):

$$\begin{aligned}\sigma_{r_m}^2 &= \begin{cases} \sigma_{x_m}^2, & m = kM + 1, \quad k = 0, 1, \dots, M-1, \\ \sigma_{x_m}^2 + \sigma_{q_{m-1}}^2, & \text{otherwise.} \end{cases} \\ \sigma_{y_m}^2 &= \begin{cases} \frac{\pi}{2} \beta^2 \sigma_{r_m}^2, & \text{for 1-bit ADCs} \\ \frac{\alpha^2 \sigma_{r_m}^2}{2} \sum_{i=1}^4 \nu_i^2 \left(\Psi\left(\frac{\sigma_{r_m}}{\sqrt{2}} \nu_i^{\text{hi}}\right) - \Psi\left(\frac{\sigma_{r_m}}{\sqrt{2}} \nu_i^{\text{lo}}\right) \right), & \text{for 2-bit ADCs} \end{cases} \\ \sigma_{q_m}^2 &= \sigma_{y_m}^2 - \sigma_{r_m}^2.\end{aligned}\quad (35)$$

Thus, the power of the m th quantizer input, $\sigma_{r_m}^2$, depends on the quantization noise powers computed up to index $m-1$. Then, the m th output power, $\sigma_{y_m}^2$, is given by (20) for one-bit ADCs and by (29) for two-bit ADCs. This allows us to compute $\sigma_{q_m}^2$, and from there $\sigma_{r_{m+1}}$, and so on. Following this process for indices $m=1$ to MN allows us to compute \mathbf{C}_q , and finally the complete \mathbf{C}_y is obtained from (31).

Thus, we can obtain the LMMSE estimate of the channel, $\hat{\mathbf{g}}$, as

$$\hat{\mathbf{g}} = \mathbf{C}_{gy} \mathbf{C}_y^{-1} \mathbf{y}, \quad (36)$$

where

$$\begin{aligned}\mathbf{C}_{gy} &= \mathbb{E}[\mathbf{g}\mathbf{y}^H] \\ &= \mathbb{E}[\mathbf{g}(\mathbf{\Phi}\mathbf{g} + \mathbf{n} + \mathbf{U}^{-1}\mathbf{q})^H] \\ &= \mathbf{C}_g \mathbf{\Phi}^H + \mathbb{E}[\mathbf{g}\mathbf{q}^H] \mathbf{U}^{-H} \\ &\approx \mathbf{C}_g \mathbf{\Phi}^H.\end{aligned}\quad (37)$$

The final approximation results because $\mathbb{E}[\mathbf{g}\mathbf{q}^H] = \mathbf{\Phi}^\dagger \mathbb{E}[\mathbf{x}\mathbf{q}^H] - \mathbf{\Phi}^\dagger \mathbb{E}[\mathbf{n}\mathbf{q}^H] \approx \mathbf{0}$, since $\mathbb{E}[\mathbf{x}\mathbf{q}^H] \approx \mathbf{0}$ and we can show that $\mathbb{E}[\mathbf{n}\mathbf{q}^H] \approx \mathbf{0}$ using an argument identical to that in Appendix A for Gaussian noise \mathbf{n} . The resulting algorithm for computing the LMMSE channel estimate for the $\Sigma\Delta$ array has low complexity and is summarized in Algorithm 1.

B. Channel Estimation Error

In order to use a performance metric that is independent of any scaling factor affecting either the real channel or its estimate, we define the normalized MSE (NMSE) as

$$\begin{aligned}\text{NMSE} &= \min_{\zeta} \frac{\mathbb{E}(\|\mathbf{g} - \zeta \hat{\mathbf{g}}\|_2^2)}{\mathbb{E}(\|\mathbf{g}\|_2^2)} \\ &= 1 - \frac{\mathbb{E}(\|\hat{\mathbf{g}}\mathbf{g}^H\|_2^2)}{\mathbb{E}(\|\mathbf{g}\|_2^2) \mathbb{E}(\|\hat{\mathbf{g}}\|_2^2)}.\end{aligned}\quad (38)$$

Algorithm 1: Channel estimation using $\Sigma\Delta$ array

- 1) Set $\beta = 1.05$ for one-bit operation. For $m = 1$ to MN , repeat:
 - (i) Update the diagonal elements of \mathbf{C}_r , $\sigma_{r_m}^2$, using (35), and $\sigma_{y_m}^2$ using (20) for one-bit ADCs and (29) for two-bit ADCs.
 - (ii) The elements of \mathbf{C}_q , $\sigma_{q_m}^2$, are updated using $\sigma_{q_m}^2 = \sigma_{y_m}^2 - \sigma_{r_m}^2$.
 - (iii) Update $\alpha_{m'}$ = $\begin{cases} \text{From (19) for one-bit } \Sigma\Delta \text{ ADCs,} \\ \text{From (28) for two-bit } \Sigma\Delta \text{ ADCs.} \end{cases}$
- 2) Obtain the complete matrix \mathbf{C}_y using (31).
- 3) Compute the output of the $\Sigma\Delta$ array as follows:
 - (i) $r_m = x_m$, for $m = kM + 1, k = 0, \dots, N - 1$.
 $r_m = x_m + e^{-j\psi} (r_{m-1} - y_{m-1})$, otherwise.
 - (ii) $y_m = \alpha_{m'} (\mathcal{Q}_m(\text{Re}(r_m)) + j\mathcal{Q}_m(\text{Im}(r_m)))$.
- 4) Estimate the channel, $\hat{\mathbf{g}}$, from (36).

This expression for the NMSE is valid for any estimator. For the particular case of LMMSE estimators, which necessarily satisfy $\mathbb{E}(\mathbf{g}\hat{\mathbf{g}}^H) = \mathbf{C}_{\hat{\mathbf{g}}}$, (38) can be expressed as

$$\text{NMSE} = \frac{\mathbb{E}(\|\mathbf{g}\|_2^2) - \mathbb{E}(\|\hat{\mathbf{g}}\|_2^2)}{\mathbb{E}(\|\mathbf{g}\|_2^2)} = \frac{\text{Tr}(\mathbf{C}_{\mathbf{g}} - \mathbf{C}_{\hat{\mathbf{g}}})}{\text{Tr}(\mathbf{C}_{\mathbf{g}})}, \quad (39)$$

where $\mathbf{C}_{\hat{\mathbf{g}}}$ is given by

$$\begin{aligned} \mathbf{C}_{\hat{\mathbf{g}}} &= \mathbb{E}[\hat{\mathbf{g}}\hat{\mathbf{g}}^H] = \mathbf{C}_g \Phi^H \mathbf{C}_y^{-1} \Phi \mathbf{C}_g \\ &= \mathbf{C}_g \Phi (\mathbf{C}_x + \mathbf{U}^{-1} \mathbf{C}_q \mathbf{U}^{-H})^{-1} \Phi^H \mathbf{C}_g. \end{aligned} \quad (40)$$

Finally, the estimation error covariance matrix is given by

$$\mathbf{C}_{\epsilon} = \mathbf{C}_g - \mathbf{C}_g \Phi (\mathbf{C}_x + \mathbf{U}^{-1} \mathbf{C}_q \mathbf{U}^{-H})^{-1} \Phi^H \mathbf{C}_g. \quad (41)$$

When the pilots are orthogonal and $N = K$, the matrices \mathbf{C}_x , \mathbf{C}_y and \mathbf{C}_q are block-diagonal with each block being identical. As a result, $\mathbf{C}_{\hat{\mathbf{g}}}$ is also block-diagonal and the k th $M \times M$ block corresponding to the covariance matrix of the estimated channel of the k th user is equal to that of the other users.

Remark: We note here that a candidate for comparison with the above estimator is an LMMSE channel estimator based on the output of a massive MIMO system with conventional two-bit quantizers. Although, as mentioned earlier, a channel estimator based on the Bussgang decomposition for one-bit ADCs has been derived in [1], no explicit analysis exists for two-bit ADCs. Consequently, to facilitate such a comparison, we derive the LMMSE channel estimator based on standard two-bit quantization of the array output. A fundamental difference between the standard and $\Sigma\Delta$ two-bit ADC case is the factor $\alpha_{m'}$. With the help of $\alpha_{m'}$, we were able to control the amplitude of the input to the adjacent array element and prevent the $\Sigma\Delta$ ADC system from becoming unstable. However, in the standard implementation, the output of the m th ADC is simply

$$y_m^{\text{std}} = \mathcal{Q}_{m'}(\text{Re}(x_m)) + j\mathcal{Q}_{m'}(\text{Im}(x_m)), \quad (42)$$

where

$$\mathcal{Q}_{m'}(\text{Re}(x_m)) = \frac{\sigma_x}{\sqrt{2}} \nu_i, \quad \text{if } x_m \in \left(\frac{\sigma_x}{\sqrt{2}} \nu_i^{\text{lo}}, \frac{\sigma_x}{\sqrt{2}} \nu_i^{\text{hi}} \right]. \quad (43)$$

As in the $\Sigma\Delta$ case, we will use an element-wise Bussgang decomposition and develop a linear model for the output. More specifically,

$$y_m^{\text{std}} = \gamma_m x_m + q_m^{\text{std}}, \quad (44)$$

where previous definitions hold for γ_m and q_m , and the coefficients γ_m are not constrained to be 1. By carrying out an analysis similar to that in Section IV, we can solve for γ_m to get

$$\gamma_m = \frac{\mathbb{E}(x_m (y_m^{\text{std}})^*)}{\mathbb{E}(|x_m|^2)} = \sum_{i=2}^4 \frac{(\nu_i - \nu_{i-1})}{\sqrt{2\pi}} \exp\left(-\frac{(\nu_i^{\text{lo}})^2}{2}\right). \quad (45)$$

The resulting expression for γ_m is independent of m , so we define $\gamma \triangleq \gamma_m$. Finally, the output power and quantization noise powers are, respectively,

$$\begin{aligned} \sigma_{y_m^{\text{std}}}^2 &= \frac{\sigma_{x_m}^2}{2} \sum_{i=1}^4 \nu_i^2 \left(\Psi\left(\frac{\sigma_{x_m}}{\sqrt{2}} \nu_i^{\text{hi}}\right) - \Psi\left(\frac{\sigma_{x_m}}{\sqrt{2}} \nu_i^{\text{lo}}\right) \right), \\ \sigma_{q_m^{\text{std}}}^2 &= \sigma_{y_m^{\text{std}}}^2 - \gamma^2 \sigma_{x_m}^2. \end{aligned} \quad (46)$$

Let the ADC outputs be stacked in \mathbf{y}^{std} . Then, defining $\mathbf{C}_{q^{\text{std}}}$ as a diagonal matrix with $\sigma_{q_m^{\text{std}}}^2$ as its elements, the complete auto-correlation matrix of \mathbf{y}^{std} is given by

$$\mathbf{C}_{y^{\text{std}}} = \gamma \mathbf{C}_x + \mathbf{C}_{q^{\text{std}}}. \quad (47)$$

The LMMSE channel estimate is then obtained by

$$\hat{\mathbf{g}}^{\text{std}} = \mathbf{C}_g \Phi^H \mathbf{C}_{y^{\text{std}}}^{-1} \mathbf{y}^{\text{std}}. \quad (48)$$

VI. UPLINK ACHIEVABLE RATE ANALYSIS

In this section, we derive the uplink achievable rate with MRC and ZF receivers. In the uplink data transmission stage, the K users transmit their data represented by the $K \times 1$ vector \mathbf{s} . Using a Bussgang decomposition as described previously on the $\Sigma\Delta$ -quantized received signal, \mathbf{y}_d , we get

$$\mathbf{y}_d = \mathcal{Q}(\mathbf{r}_d) = \sqrt{\rho_d} \mathbf{G} \mathbf{s} + \mathbf{n}_d + \mathbf{U}_d^{-1} \mathbf{q}_d, \quad (49)$$

where $\mathbf{r}_d = \mathbf{U}_d (\sqrt{\rho_d} \mathbf{G} \mathbf{s} + \mathbf{n}_d) - \mathbf{V}_d \mathbf{y}_d$, ρ_d is the data transmission power, \mathbf{n}_d and \mathbf{q}_d are the noise and quantization noise in the data phase, respectively. The matrices \mathbf{U}_d and \mathbf{V}_d are defined by taking $N = 1$ in Eq. (10). We assume that the user symbols s_k are i.i.d with $\mathbb{E}[|s_k|^2] = 1$ and the noise vector \mathbf{n} consists of zero-mean circularly symmetric white Gaussian random variables with variance 1. In the derivation of the achievable rate, we will assume that during the training phase, the pilots are orthogonal and that $N = K$. Consequently, the matrices \mathbf{C}_x , \mathbf{C}_y and $\mathbf{C}_{\hat{\mathbf{g}}}$ will be block-diagonal.

Additionally, the analysis of the achievable rate relies on the covariance matrix of \mathbf{q}_d , \mathbf{C}_{q_d} , which is different from the quantization noise covariance matrix of the training phase. For the data transmission stage, this matrix has to be derived in a manner similar to Section V. Inspecting the recursion equations developed in the previous section, we see that initialization of the recursion will be performed with \mathbf{C}_{x_d} , where $\mathbf{C}_{x_d} = \rho_d \mathbf{G} \mathbf{G}^H + \mathbf{I}$. In order to perform the Bussgang

decomposition, the matrix $\mathbf{G}\mathbf{G}^H$ should be known in advance. However, we can leverage the inherent channel hardening in massive MIMO systems to assume that $\mathbf{H}\mathbf{H}^H \approx K\mathbf{I}$. Thus,

$$\mathbf{C}_{x_d} \approx K\rho_d\mathbf{C}_G + \mathbf{I}. \quad (50)$$

The above approximation does not require perfect CSI and this technique has been used in related prior work (*e.g.*, see [1], [3]).

The procedure to obtain \mathbf{C}_{q_d} is outlined as follows. Let $\sigma_{r_{dm}}^2$, $\sigma_{y_{dm}}^2$ and $\sigma_{q_{dm}}^2$ denote the powers of the m th components of \mathbf{r}_d , \mathbf{y}_d and \mathbf{q}_d , respectively. Then, (35) is modified for the data transmission stage as

$$\sigma_{r_{dm}}^2 = \begin{cases} \sigma_{x_d}^2, & m = 0, 1, \dots, M, \\ \sigma_{x_d}^2 + \sigma_{q_{d_{m-1}}}^2, & \text{otherwise.} \end{cases}$$

$$\sigma_{y_{dm}}^2 = \begin{cases} \frac{\pi}{2}\beta^2\sigma_{r_{dm}}^2, & \text{for 1-bit ADCs} \\ \frac{\alpha^2\sigma_{r_{dm}}^2}{2} \sum_{i=1}^4 \nu_i^2 \left(\Psi\left(\frac{\sigma_{r_{dm}}}{\sqrt{2}}\nu_i^{\text{hi}}\right) - \Psi\left(\frac{\sigma_{r_{dm}}}{\sqrt{2}}\nu_i^{\text{lo}}\right) \right), & \text{for 2-bit ADCs} \end{cases}$$

$$\sigma_{q_{dm}}^2 = \sigma_{y_{dm}}^2 - \sigma_{r_{dm}}^2, \quad (51)$$

where $\sigma_{x_d}^2 = K\rho_d + 1$ since \mathbf{C}_G is equal to $\mathbf{A}\mathbf{A}^H/L$ and its diagonal elements are equal to unity. The diagonal matrix \mathbf{C}_{q_d} is completed with $\sigma_{q_{dm}}^2$ as its diagonal elements.

The BS uses a linear receiver for symbol detection that depends on the LMMSE channel estimate. Denoting the linear receiver by \mathbf{W} , the detected symbol vector is obtained by multiplying the conjugate transpose of \mathbf{W} with the received signal vector as

$$\hat{\mathbf{s}} = \mathbf{W}^H \mathbf{y}_d = \sqrt{\rho_d} \mathbf{W}^H \mathbf{G} \mathbf{s} + \mathbf{W}^H \mathbf{n}_d + \mathbf{W}^H \mathbf{U}_d^{-1} \mathbf{q}_d. \quad (52)$$

We consider the performance of two linear receivers in particular, namely the MRC and ZF receivers, where \mathbf{W} is given by

$$\begin{aligned} \mathbf{W}_{\text{MRC}} &= \hat{\mathbf{G}} \\ \mathbf{W}_{\text{ZF}} &= \hat{\mathbf{G}} \left(\hat{\mathbf{G}}^H \hat{\mathbf{G}} \right)^{-1}. \end{aligned} \quad (53)$$

Here, $\hat{\mathbf{G}}$ is the $M \times K$ matrix formed from $\hat{\mathbf{g}}$ using the inverse of the *vec* operation. From (52), we can re-write the various components contributing to the k th detected symbol as

$$\begin{aligned} \hat{s}_k &= \sqrt{\rho_d} \mathbb{E} \left[\mathbf{w}_k^H \mathbf{g}_k \right] s_k + \sqrt{\rho_d} \left(\mathbf{w}_k^H \mathbf{g}_k - \mathbb{E} \left[\mathbf{w}_k^H \mathbf{g}_k \right] \right) s_k + \\ &\quad \sqrt{\rho_d} \mathbf{w}_k^H \sum_{i \neq k} \mathbf{g}_i s_i + \mathbf{w}_k^H \mathbf{n}_d + \mathbf{w}_k^H \mathbf{U}_d^{-1} \mathbf{q}_d, \end{aligned} \quad (54)$$

where \mathbf{w}_k is the k th column of \mathbf{W} . The terms in the above equation correspond to the desired signal, the receiver uncertainty, the inter-user interference, the additive noise and the quantization noise, respectively. We will follow an approach similar to [3] and [42] and use the classical worst-case uncorrelated Gaussian assumption on the terms in (54) to obtain a lower bound on the achievable rate. Treating the

final four terms as ‘‘effective noise’’, the achievable rate of the k th user is given by (55) at the top of the next page. Whereas the achievable rate bounds derived in [32] assume perfect knowledge of the CSI, our result takes into account the channel estimation error. In our derivation of the worst-case bound, we assume that the channel estimate $\hat{\mathbf{g}}$ is Gaussian with covariance matrix $\mathbf{C}_{\hat{g}}$ given by (40). Similarly, \mathbf{q}_d is also assumed to be Gaussian and its covariance matrix is obtained as described earlier in this section.

A. MRC receiver

For a massive MIMO system with a spatial $\Sigma\Delta$ array and an MRC receiver based on the LMMSE channel estimate, the achievable rate of the k th user is given by (56) on the next page. To show this, we compute below the individual terms in the achievable rate expression of (55).

$$\begin{aligned} \mathbb{E} \left[\hat{\mathbf{g}}_k^H \mathbf{g}_k \right] &= \mathbb{E} \left[\hat{\mathbf{g}}_k^H (\hat{\mathbf{g}}_k + \boldsymbol{\epsilon}_k) \right] \\ &= \mathbb{E} \left[\|\hat{\mathbf{g}}_k\|^2 \right] + \mathbb{E} \left[\hat{\mathbf{g}}_k^H \boldsymbol{\epsilon}_k \right] \\ &= \mathbb{E} \left[\|\hat{\mathbf{g}}_k\|^2 \right] = \text{Tr}(\mathbf{C}_{\hat{g}_k}) = \frac{\text{Tr}(\mathbf{C}_{\hat{g}})}{K}, \end{aligned}$$

where we have used the fact that the LMMSE channel estimate is uncorrelated with the channel estimation error and that the covariance matrices of the estimated channels for each of the users are equal. Further,

$$\begin{aligned} \text{var}(\hat{\mathbf{g}}_k^H \mathbf{g}_k) &= \mathbb{E} \left[\left| \hat{\mathbf{g}}_k^H \mathbf{g}_k \right|^2 \right] - \left(\mathbb{E} \left[\hat{\mathbf{g}}_k^H \mathbf{g}_k \right] \right)^2 \\ &= \mathbb{E} \left[\left| \|\hat{\mathbf{g}}_k\|^2 + \hat{\mathbf{g}}_k^H \boldsymbol{\epsilon}_k \right|^2 \right] - \left(\mathbb{E} \left[\hat{\mathbf{g}}_k^H \mathbf{g}_k \right] \right)^2 \\ &= \mathbb{E} \left[\|\hat{\mathbf{g}}_k\|^4 \right] + \mathbb{E} \left[\|\hat{\mathbf{g}}_k\|^2 \hat{\mathbf{g}}_k^H \boldsymbol{\epsilon}_k \right] + \mathbb{E} \left[\|\hat{\mathbf{g}}_k\|^2 \boldsymbol{\epsilon}_k^H \hat{\mathbf{g}}_k \right] + \\ &\quad \mathbb{E} \left[\|\hat{\mathbf{g}}_k^H \boldsymbol{\epsilon}_k\|^2 \right] - \left(\mathbb{E} \left[\hat{\mathbf{g}}_k^H \mathbf{g}_k \right] \right)^2 \\ &= 2 \left(\mathbb{E} \left[\|\hat{\mathbf{g}}_k\|^2 \right] \right)^2 + \mathbb{E} \left[\|\hat{\mathbf{g}}_k\|^2 \right] \mathbb{E} \left[\|\boldsymbol{\epsilon}_k\|^2 \right] - \left(\mathbb{E} \left[\hat{\mathbf{g}}_k^H \mathbf{g}_k \right] \right)^2 \\ &= \left(\text{Tr}(\mathbf{C}_{\hat{g}_k}) \right)^2 + \text{Tr}(\mathbf{C}_{\hat{g}_k}) \left[\text{Tr}(\mathbf{C}_G) - \text{Tr}(\mathbf{C}_{\hat{g}_k}) \right] \\ &= \text{Tr}(\mathbf{C}_{\hat{g}_k}) \text{Tr}(\mathbf{C}_G) = \frac{\text{Tr}(\mathbf{C}_{\hat{g}}) \text{Tr}(\mathbf{C}_G)}{K}, \end{aligned}$$

and, for $i \neq k$,

$$\begin{aligned} \mathbb{E} \left[\left| \hat{\mathbf{g}}_k^H \mathbf{g}_i \right|^2 \right] &= \left| \mathbb{E} \left[\hat{\mathbf{g}}_k^H \mathbf{g}_i \right] \right|^2 + \mathbb{E} \left[\|\hat{\mathbf{g}}_k\|^2 \right] \mathbb{E} \left[\|\mathbf{g}_i\|^2 \right], \\ \mathbb{E} \left[\hat{\mathbf{g}}_k^H \mathbf{g}_i \right] &= \mathbb{E} \left[\left(\mathbf{P}_k \boldsymbol{\Phi} \mathbf{g} + \mathbf{P}_k \mathbf{n} + \mathbf{P}_k \mathbf{U}^{-1} \mathbf{q} \right)^H \mathbf{g}_i \right], \end{aligned}$$

where $\mathbf{P}_k = \mathbf{C}_{g^{(k-1)M:kM}} \boldsymbol{\Phi} \mathbf{C}_y^{-1}$ and $\mathbf{C}_{g^{(k-1)M:kM}}$ refers to the k th block of rows of \mathbf{C}_g , and where we have substituted the expression for $\hat{\mathbf{g}}_k$ in the above equation. Then, using the fact that \mathbf{g}_i is uncorrelated with the quantization noise and the additive noise, we get

$$\mathbb{E} \left[\left| \hat{\mathbf{g}}_k^H \mathbf{g}_i \right|^2 \right] = \frac{\text{Tr}(\mathbf{C}_{\hat{g}}) \text{Tr}(\mathbf{C}_G)}{K}.$$

We can solve for the final term in the denominator in a similar manner to get:

$$\mathbb{E} \left[\left| \hat{\mathbf{g}}_k^H \mathbf{U}_d^{-1} \mathbf{q} \right|^2 \right] = \frac{\text{Tr}(\mathbf{C}_{\hat{g}}) \text{Tr}(\mathbf{U}_d^{-1} \mathbf{C}_{q_d} \mathbf{U}_d^{-H})}{K}.$$

Note that when there is perfect knowledge of the CSI, *i.e.* $\mathbf{w}_k = \mathbf{g}_k$, (56) reduces to the expression in [32].

$$R_k = \log_2 \left(1 + \frac{\rho_d \mathbb{E} [\mathbf{w}_k^H \mathbf{g}_k]^2}{\rho_d \text{var}(\mathbf{w}_k^H \mathbf{g}_k) + \rho_d \sum_{i \neq k} \mathbb{E} [|\mathbf{w}_k^H \mathbf{g}_i|^2] + \mathbb{E} [|\mathbf{w}_k^H \mathbf{n}_d|^2] + \mathbb{E} [|\mathbf{w}_k^H \mathbf{U}_d^{-1} \mathbf{q}_d|^2]} \right) \quad (55)$$

$$R_k^{\text{MRC}} = \log_2 \left(1 + \frac{\rho_d (\text{Tr}(\mathbf{C}_{\hat{g}}))^2 / K}{\rho_d K \text{Tr}(\mathbf{C}_{\hat{g}}) \text{Tr}(\mathbf{C}_G) + \text{Tr}(\mathbf{C}_{\hat{g}}) + \text{Tr}(\mathbf{C}_{\hat{g}}) \text{Tr}(\mathbf{U}_d^{-1} \mathbf{C}_{q_d} \mathbf{U}_d^{-H})} \right) \quad (56)$$

B. ZF receiver

For the zero-forcing case, the expectations of the individual terms are more complicated and difficult to evaluate in closed-form. The achievable rate of the k th user is given by (58), where the term $\mathbb{E} \left[\left(\hat{\mathbf{G}}^H \hat{\mathbf{G}} \right)_{kk} \right]$ is computed empirically. The remaining terms in the expression are computed as follows. For the numerator,

$$\mathbb{E} [\mathbf{w}_k^H \mathbf{g}_k] = \mathbb{E} [\mathbf{w}_k^H (\hat{\mathbf{g}}_k + \boldsymbol{\epsilon}_k)] = 1 + \mathbb{E} [\mathbf{w}_k^H \boldsymbol{\epsilon}_k] = 1. \quad (57)$$

Further,

$$\text{var}(\mathbf{w}_k^H \mathbf{g}_k) = \mathbb{E} [\|\mathbf{w}_k^H \boldsymbol{\epsilon}_k\|^2] = \frac{\mathbb{E} \left[\left(\hat{\mathbf{G}}^H \hat{\mathbf{G}} \right)_{kk} \right] \text{Tr}(\mathbf{C}_\epsilon)}{K}.$$

For $i \neq k$, we have

$$\mathbb{E} [|\mathbf{w}_k^H \mathbf{g}_i|^2] = \mathbb{E} [|\mathbf{w}_k^H \boldsymbol{\epsilon}_i|^2] = \frac{\mathbb{E} \left[\left(\hat{\mathbf{G}}^H \hat{\mathbf{G}} \right)_{kk} \right] \text{Tr}(\mathbf{C}_\epsilon)}{K}.$$

Similarly, we obtain

$$\begin{aligned} \mathbb{E} [|\mathbf{w}_k^H \mathbf{n}_d|^2] &= \mathbb{E} \left[\left(\hat{\mathbf{G}}^H \hat{\mathbf{G}} \right)_{kk}^{-1} \right], \\ \mathbb{E} [|\mathbf{w}_k^H \mathbf{U}_d^{-1} \mathbf{q}_d|^2] &= \mathbb{E} \left[\left(\hat{\mathbf{G}}^H \hat{\mathbf{G}} \right)_{kk}^{-1} \right] \text{Tr}(\mathbf{U}_d^{-1} \mathbf{C}_{q_d} \mathbf{U}_d^{-H}). \end{aligned}$$

VII. SIMULATION RESULTS

In this section, we numerically evaluate the NMSE and sum spectral efficiency achieved with the $\Sigma\Delta$ massive MIMO system with both one and two-bit outputs. All simulations will employ a uniform linear array (ULA) equipped with 128 antennas, the number of pilot symbols and number of users are both 10 ($N = K = 10$), and orthogonal pilot sequences are used based on the $N \times N$ DFT matrix. Therefore, ρ represents the per user and per antenna SNR. We further assume that the downlink transmission power is equal to the pilot transmission power, i.e. $\rho_d = \rho$. The users are located within a sector near the broadside of the antenna array with variable angular spread per user, Θ , so the steering angle of the $\Sigma\Delta$ array is set to 0° . The number of coherent paths per user within the sector, L , is 50. Thus, the channel is spatially correlated and \mathbf{C}_g is non-diagonal. The NMSE of the channel estimate is evaluated over 500 independent realizations of the channel. For two-bit ADCs, we choose the optimum levels $\{\nu_1, \nu_2, \nu_3, \nu_4\}$ as per [39]. We also use the sum spectral efficiency as a performance measure defined as

$$\text{SE} = \frac{T - N}{T} \sum_{i=1}^K R_k, \quad (59)$$

where T is length of the coherence interval during which the channel remains constant. We assume that $T = 200$ symbols.

We compare the performance of the $\Sigma\Delta$ LMMSE channel estimator derived in this paper with the standard one-bit Bussgang LMMSE (BLMMSE) channel estimator of [1] and the LMMSE channel estimator derived for standard two-bit quantization in Section V. The NMSE of an LMMSE channel estimator using unquantized measurements is also evaluated. Fig. 2 shows the channel estimation performance as a function of the angular spread of the user AoAs for four different antenna spacings. As expected, the performance of the spatial $\Sigma\Delta$ approach improves as either the antenna spacing δ or the size of the users' angular spread Θ decreases. Without oversampling, i. e., when $\delta = \lambda/2$, the $\Sigma\Delta$ array offers no benefit over regular one- and two-bit quantization, except for a very narrow region near broadside. For $\delta \leq \lambda/4$, however, there is a significant gain for angular sectors up to 90° and beyond. For the remaining simulation examples, we will set $\Theta = 60^\circ$ and $\delta = \lambda/6$.

Fig. 3 shows the NMSE of the channel estimates as a function of SNR with $M = 128$ antennas. The solid lines show the NMSE predicted by (39), while the symbols indicate the simulation results (this convention will be followed in all subsequent plots). We see that there is excellent agreement between our theoretical expression and the simulations. At low-to-medium SNRs, the performance of the $\Sigma\Delta$ channel estimates is very close to that of the unquantized MMSE channel estimate. The NMSE with two-bit $\Sigma\Delta$ ADCs is also lower than that achieved by one-bit $\Sigma\Delta$ ADCs beyond an SNR of -5dB . The gap between the two widens as the SNR increases and the error floor is about -15dB with one-bit $\Sigma\Delta$ ADCs and -18dB with two-bit $\Sigma\Delta$ ADCs. It is seen that LMMSE channel estimation with the $\Sigma\Delta$ array offers a significant advantage over the conventional one-bit and two-bit quantized arrays. The error floor with $\Sigma\Delta$ channel estimators is around 8dB lower than their counterparts employing standard quantization. The gain of the spatial $\Sigma\Delta$ approach is plotted as a function of M for a fixed SNR of 0dB in Fig. 4.

In Fig. 5, we plot the theoretical and simulated sum spectral efficiency (SE) achieved by MRC and ZF receivers using the LMMSE channel estimate. Fig. 5(a) shows that the SE of the $\Sigma\Delta$ architectures is close to that of an unquantized system and a bit higher than that of the one-bit massive MIMO system, although for MRC the difference in SE is not so large since multi-user interference is more of a limiting factor. There is excellent agreement between the simulations and our analytical expression in (56). More impressive results are obtained for the case of a ZF receiver, as shown in Fig. 5(b). At

$$R_k^{\text{ZF}} = \log_2 \left(1 + \frac{\rho_d}{\rho_d \mathbb{E} \left[\left(\hat{\mathbf{G}}^H \hat{\mathbf{G}} \right)_{kk}^{-1} \right] \text{Tr}(\mathbf{C}_\epsilon) + \mathbb{E} \left[\left(\hat{\mathbf{G}}^H \hat{\mathbf{G}} \right)_{kk}^{-1} \right] + \mathbb{E} \left[\left(\hat{\mathbf{G}}^H \hat{\mathbf{G}} \right)_{kk}^{-1} \right] \text{Tr}(\mathbf{U}_d^{-1} \mathbf{C}_{q_d} \mathbf{U}_d^{-H})} \right) \quad (58)$$

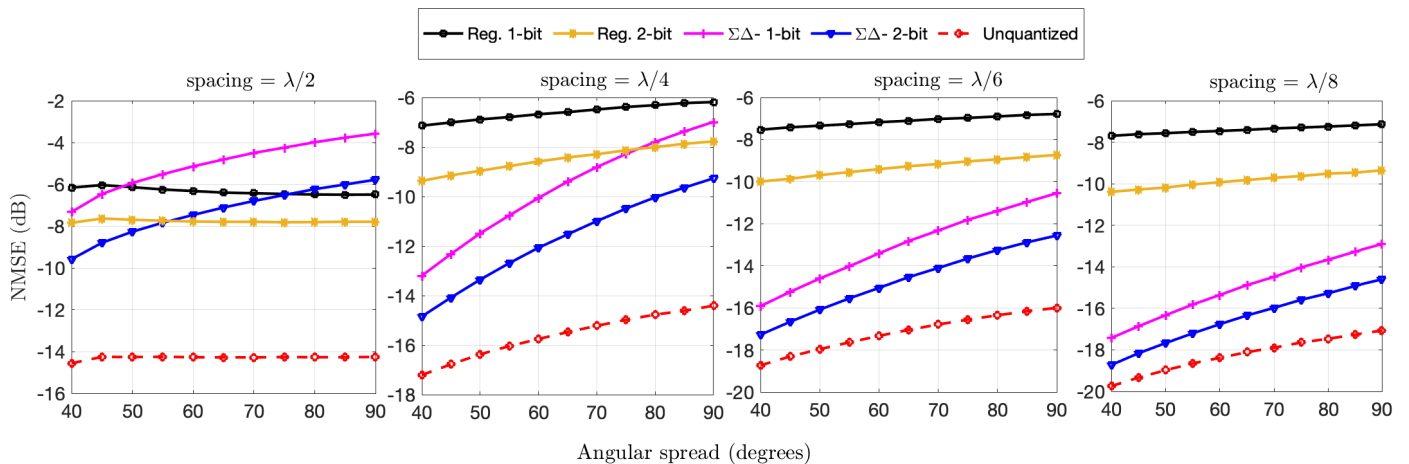


Fig. 2: NMSE of channel estimates for different angular spreads of user AoAs and inter-element antenna spacings.

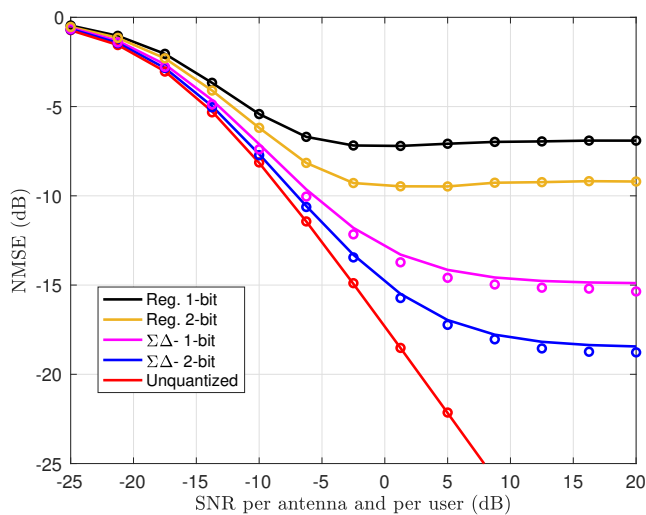


Fig. 3: NMSE of channel estimate, $M = 128$, $N = K = 10$. The theoretical values are indicated by solid lines whereas the simulated values are denoted by circles.

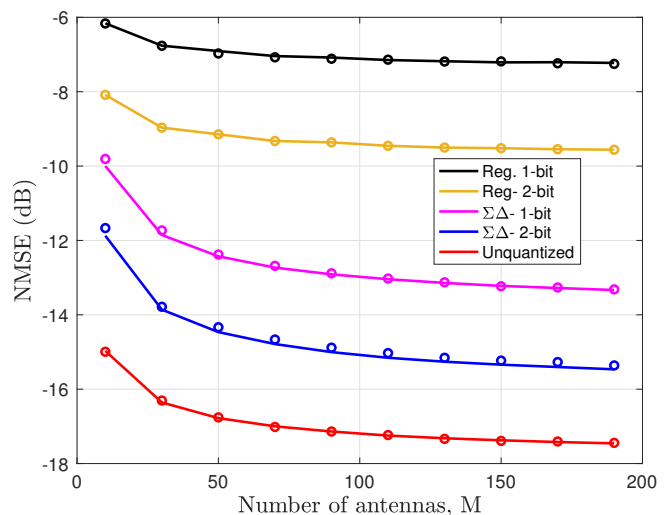
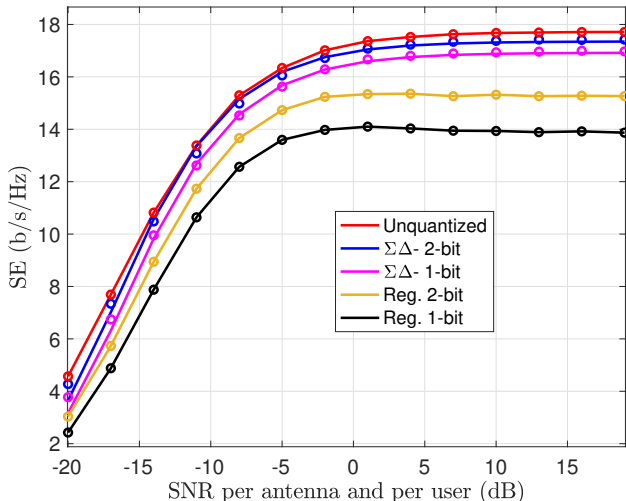


Fig. 4: NMSE of channel estimate as a function of the number of antennas, $\text{SNR} = 0\text{dB}$.

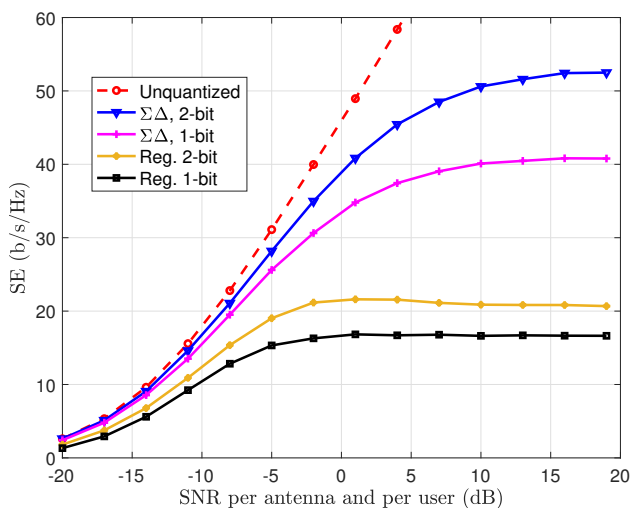
high SNRs, the throughput achieved with two-bit $\Sigma\Delta$ ADCs is around 50 bits/s/Hz, almost 2.5 times that achieved with regular two-bit ADCs. With one-bit $\Sigma\Delta$ ADCs, the maximum throughput is around 40 bits/s/Hz, around twice that achieved with regular one-bit ADCs. Of course, there is also a much bigger gap between the spectral efficiencies achievable by the $\Sigma\Delta$ and unquantized systems as well, especially at high SNR.

Finally, Fig. 6 shows a plot of the average per-user achievable rate for the MRC (solid lines) and ZF (dashed lines)

receivers versus the total number of users. For MRC, the per-user rate achieved with both the one-bit and two-bit $\Sigma\Delta$ ADC arrays is essentially identical to that achieved without quantization. The numerator term of the log term in (56) decreases with K while the inter-user interference term in the denominator increases K . The net effect is that, as the number of uplink users increases, the effective SNR per user for MRC decreases as $O(K^2)$. The per-user rate for ZF is significantly higher, with the $\Sigma\Delta$ architecture falling in between the standard one-bit and unquantized systems. For



(a)



(b)

Fig. 5: Sum spectral efficiency (SE) with (a) MRC (b) ZF receivers ($M = 128, K = 10$).

an average per-user rate of 2 bits/s/Hz, MRC can support 7-8 users almost independently of the quantization level, while for ZF the number of users increases to 8-11 for standard one- and two-bit quantization, 18-20 for the $\Sigma\Delta$ array, and 23 without quantization. As the number of users increases, the channel matrix becomes ill-conditioned and the sum rate achieved with the ZF receiver tends towards zero. This is partially due to the fact that the users' signals are confined to arrive from a certain angular sector (in this case, a 60° sector), and could be ameliorated using an MMSE receiver.

VIII. CONCLUSION

In this paper, we considered channel estimation in massive MIMO systems employing spatial $\Sigma\Delta$ modulation with one- or two-bit ADCs. We used an element-wise Busgang decomposition to derive a new LMMSE channel estimator that takes into account the effect of the correlation between the

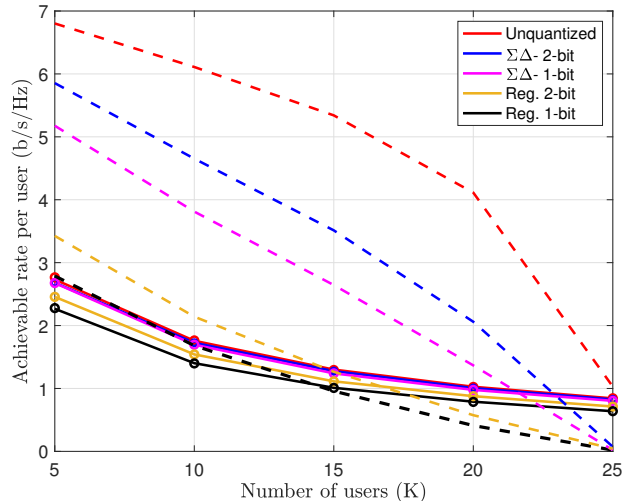


Fig. 6: Per-user achievable rate as a function of the number of users, $\text{SNR} = 5\text{dB}$, $M = 128$. Solid lines indicate results with MRC receiver while the results for ZF receiver are plotted with dashed lines of same color.

quantizer outputs. We further analyzed the uplink rate that is achievable for MRC and ZF linear receivers implemented with the LMMSE channel estimate. The simulation results show that, in situations where the users are confined to a certain angular sector or the array elements are more closely spaced than one-half wavelength, the spatial $\Sigma\Delta$ approach is able to achieve significantly better channel estimates and spectral efficiency than systems employing direct quantization using one- and two-bit ADCs. At low-to-medium SNR values, the performance gap the $\Sigma\Delta$ array and a system with infinite-resolution ADCs is negligible. We derived a theoretical expressions for the channel estimation error and lower bounds on the achievable spectral efficiency, and showed that they provided excellent predictions for the performance obtained numerically. Overall, our results indicate that the spatial $\Sigma\Delta$ architecture provides a promising approach for increasing the energy efficiency and reducing the hardware complexity of large-scale antenna systems.

APPENDIX A

We will prove that $\mathbb{E}[x_m q_n^*] \approx 0, \forall m, n$ following an approach similar to that in Appendix A of [1]. We can express $\mathbb{E}[x_m q_n^*]$ as

$$\mathbb{E}[x_m q_n^*] = \mathbb{E}_{r_n} [\mathbb{E}[x_m q_n^* | r_n]] = \mathbb{E}_{r_n} [\mathbb{E}[x_m | r_n] q_n^*], \quad (60)$$

where the last equality follows from the fact that $q_n = y_n - r_n$ is fixed for a given r_n . $\mathbb{E}[x_m | r_n]$ is the MMSE estimate of x_m given r_n . Since we assume that r_n is approximately a Gaussian random variable, the MMSE estimate of the Gaussian variable x_m will be approximately equivalent to the LMMSE estimate given by

$$\mathbb{E}[x_m | r_n] \approx \frac{\mathbb{E}[x_m r_n^*]}{\sigma_{r_n}^2} r_n. \quad (61)$$

Using (61) and the fact that r_n is uncorrelated with q_n , we have

$$\mathbb{E}[x_m q_n^*] \approx \frac{\mathbb{E}[x_m r_n^*]}{\sigma_{r_n}^2} \mathbb{E}_{r_n}[r_n q_n^*] = 0. \quad (62)$$

Therefore, $\mathbb{E}[x_m q_n^*] \approx 0, \forall m, n$ and hence $\mathbb{E}[\mathbf{xq}^H] \approx \mathbf{0}$.

REFERENCES

- [1] Y. Li, C. Tao, G. Seco-Granados, A. Mezghani, A. L. Swindlehurst, and L. Liu, "Channel estimation and performance analysis of one-bit massive MIMO systems," *IEEE Trans. Signal Process.*, vol. 65, no. 15, pp. 4075–4089, August 2017.
- [2] S. Jacobsson, G. Durisi, M. Coldrey, U. Gustavsson, and C. Studer, "Throughput analysis of massive MIMO uplink with low-resolution ADCs," *IEEE Trans. Wireless Commun.*, vol. 16, no. 6, pp. 4038–4051, June 2017.
- [3] C. Mollén, J. Choi, E. G. Larsson, and R. W. Heath, "Uplink performance of wideband massive MIMO with one-bit ADCs," *IEEE Trans. Wireless Commun.*, vol. 16, no. 1, pp. 87–100, Jan 2017.
- [4] J. Choi, J. Mo, and R. W. Heath, "Near maximum-likelihood detector and channel estimator for uplink multiuser massive MIMO systems with one-bit ADCs," *IEEE Trans. Commun.*, vol. 64, no. 5, pp. 2005–2018, May 2016.
- [5] Y.-S. Jeon, N. Lee, S.-N. H., and R. W. Heath, "One-bit sphere decoding for uplink massive MIMO systems with one-bit ADCs," *IEEE Trans. Wireless Commun.*, vol. 17, no. 7, pp. 4509–4521, 2018.
- [6] P. Dong, H. Zhang, W. Xu, G. Y. Li, and X. You, "Performance analysis of multiuser massive MIMO with spatially correlated channels using low-precision ADC," *IEEE Commun. Lett.*, vol. 22, no. 1, pp. 205–208, 2017.
- [7] A. Mezghani, R. Ghiat, and J. A. Nossek, "Transmit processing with low resolution D/A-converters," in *IEEE Int. Conf. on Electronics, Circuits and Systems (ICECS 2009)*. IEEE, 2009, pp. 683–686.
- [8] Y. Li, C. Tao, A. L. Swindlehurst, A. Mezghani, and L. Liu, "Downlink achievable rate analysis in massive MIMO systems with one-bit DACs," *IEEE Commun. Lett.*, vol. 21, no. 7, pp. 1669–1672, 2017.
- [9] S. Jacobsson, G. Durisi, M. Coldrey, and C. Studer, "Massive MU-MIMO-OFDM downlink with one-bit DACs and linear precoding," in *Proc. Globecom*. IEEE, 2017.
- [10] A. K. Saxena, I. Fijalkow, and A. L. Swindlehurst, "Analysis of one-bit quantized precoding for the multiuser massive MIMO downlink," *IEEE Trans. Signal Process.*, vol. 65, no. 17, pp. 4624–4634, 2017.
- [11] H. Jedda, A. Mezghani, A. L. Swindlehurst, and J. A. Nossek, "Quantized constant envelope precoding with PSK and QAM signaling," *IEEE Trans. Wireless Commun.*, vol. 17, no. 12, pp. 8022–8034, 2018.
- [12] L. T. N. Landau and R. C. de Lamare, "Branch-and-bound precoding for multiuser MIMO systems with 1-bit quantization," *IEEE Wireless Commun. Lett.*, vol. 6, no. 6, pp. 770–773, 2017.
- [13] J. García, J. Munir, K. Roth, and J. A. Nossek, "Channel estimation and data equalization in frequency-selective MIMO systems with one-bit quantization," *arXiv preprint arXiv:1609.04536*, 2016.
- [14] S. Jacobsson, G. Durisi, M. Coldrey, U. Gustavsson, and C. Studer, "One-bit massive MIMO: Channel estimation and high-order modulations," in *Proc. IEEE Int. Conf. on Commun. Workshop (ICCW)*. IEEE, 2015, pp. 1304–1309.
- [15] O. Mehanna and N. D. Sidiropoulos, "Channel tracking and transmit beamforming with frugal feedback," *IEEE Trans. Signal Process.*, vol. 62, no. 24, pp. 6402–6413, 2014.
- [16] O. Dabeer and U. Madhow, "Channel estimation with low-precision analog-to-digital conversion," in *Proc. ICC*. IEEE, 2010.
- [17] K. Roth, H. Pirzadeh, A. L. Swindlehurst, and J. A. Nossek, "A comparison of hybrid beamforming and digital beamforming with low-resolution ADCs for multiple users and imperfect CSI," *IEEE J. Sel. Topics Sig. Proc.*, vol. 12, no. 3, pp. 484–498, June 2018.
- [18] H. Pirzadeh and A. L. Swindlehurst, "Spectral efficiency under energy constraint for mixed-ADC MRC massive MIMO," *IEEE Signal Process. Lett.*, vol. 24, no. 12, pp. 1847–1851, 2017.
- [19] A. B. Üçüncü and A. Ö. Yılmaz, "Oversampling in one-bit quantized massive MIMO systems and performance analysis," *IEEE Trans. Wireless Commun.*, vol. 17, no. 12, pp. 7952–7964, Dec. 2018.
- [20] A. Gokceoglu, E. Björnson, E. G. Larsson, and M. Valkama, "Spatio-temporal waveform design for multiuser massive MIMO downlink with 1-bit receivers," *IEEE J. Sel. Topics Sig. Proc.*, vol. 11, no. 2, pp. 347–362, March 2017.
- [21] M. Schluter, M. Dörpinghaus, and G. P. Fettweis, "Bounds on channel parameter estimation with 1-bit quantization and oversampling," in *Proc. IEEE. Int. Workshop on Sig. Proc. Advances in Wireless Communications (SPAWC)*, June 2018.
- [22] P. M. Aziz, H. V. Sorensen, and J. Van der Spiegel, "An overview of sigma-delta converters," *IEEE Signal Process. Mag.*, vol. 13, no. 1, pp. 61–84, 1996.
- [23] R. Gray, "Oversampled sigma-delta modulation," *IEEE Trans. Commun.*, vol. 35, no. 5, pp. 481–489, 1987.
- [24] R. M. Gray, W. Chou, and P. W. Wong, "Quantization noise in single-loop sigma-delta modulation with sinusoidal inputs," *IEEE Trans. Commun.*, vol. 37, no. 9, pp. 956–968, Sep 1989.
- [25] S. H. Ardalan, "Analysis of delta-sigma modulators with bandlimited Gaussian inputs," in *Proc. ICASSP*, April 1988, pp. 1866–1869 vol.3.
- [26] D. S. Palguna, D. J. Love, T. A. Thomas, and A. Ghosh, "Millimeter wave receiver design using low precision quantization and parallel $\Delta\Sigma$ architecture," *IEEE Trans. Wireless Commun.*, vol. 15, no. 10, pp. 6556–6569, Oct 2016.
- [27] V. Venkateswaran and A. van der Veen, "Multichannel $\Sigma\Delta$ ADCs with integrated feedback beamformers to cancel interfering communication signals," *IEEE Trans. Signal Process.*, vol. 59, no. 5, pp. 2211–2222, May 2011.
- [28] R. M. Corey and A. C. Singer, "Spatial sigma-delta signal acquisition for wideband beamforming arrays," in *Proc. Int. ITG Workshop on Smart Antennas*, March 2016.
- [29] D. Barac and E. Lindqvist, "Spatial sigma-delta modulation in a massive MIMO cellular system," M.S. thesis, Department of Computer Science and Engineering, Chalmers University of Technology, 2016.
- [30] S. Rao, A. L. Swindlehurst, and H. Pirzadeh, "Massive MIMO channel estimation with 1-bit spatial sigma-delta ADCs," in *Proc. ICASSP*. IEEE, 2019, pp. 4484–4488.
- [31] M. Shao, W. Ma, Q. Li, and A. L. Swindlehurst, "One-bit sigma-delta MIMO precoding," *IEEE J. Sel. Topics Sig. Proc.*, vol. 13, no. 5, pp. 1046–1061, Sep. 2019.
- [32] H. Pirzadeh, G. Seco-Granados, S. Rao, and A. L. Swindlehurst, "Spectral efficiency of one-bit sigma-delta massive MIMO," *arXiv preprint arXiv:1910.05491*, 2019.
- [33] D. P. Scholnik, J. O. Coleman, D. Bowling, and M. Neel, "Spatio-temporal delta-sigma modulation for shared wideband transmit arrays," in *Proc. Radar Conf.* IEEE, 2004, pp. 85–90.
- [34] J. D. Krieger, C. P. Yeang, and G. W. Wornell, "Dense delta-sigma phased arrays," *IEEE Trans. Antennas Propag.*, vol. 61, no. 4, pp. 1825–1837, April 2013.
- [35] A. Madanayake, N. Akram, S. Mandal, J. Liang, and L. Belostotski, "Improving ADC figure-of-merit in wideband antenna array receivers using multidimensional space-time delta-sigma multiport circuits," in *Int. Workshop on Multidimensional (nD) Sys. (nDS)*, Sept 2017.
- [36] A. Nikoofard, J. Liang, M. Twieg, S. Handagala, A. Madanayake, L. Belostotski, and S. Mandal, "Low-complexity N-port ADCs using 2-D sigma-delta noise-shaping for N-element array receivers," in *Int. Midwest Symp. on Circuits and Systems (MWSCAS)*, Aug 2017, pp. 301–304.
- [37] S. Ardalan and J. Paulos, "An analysis of nonlinear behavior in delta-sigma modulators," *IEEE Trans. Circuits Syst.*, vol. 34, no. 6, pp. 593–603, June 1987.
- [38] P. W. Wong and R. M. Gray, "Sigma-delta modulation with i.i.d. Gaussian inputs," *IEEE Trans. Inf. Theory*, vol. 36, no. 4, pp. 784–798, July 1990.
- [39] J. Max, "Quantizing for minimum distortion," *IRE Trans. on Inf. Theory*, vol. 6, no. 1, pp. 7–12, 1960.
- [40] S. Lloyd, "Least squares quantization in PCM," *IEEE Trans. Inf. Theory*, vol. 28, no. 2, pp. 129–137, 1982.
- [41] R. Price, "A useful theorem for nonlinear devices having Gaussian inputs," *IRE Trans. Inf. Theory*, vol. 4, no. 2, pp. 69–72, 1958.
- [42] Q. Zhang, S. Jin, K.-K. Wong, H. Zhu, and M. Matthaiou, "Power scaling of uplink massive MIMO systems with arbitrary-rank channel means," *IEEE Trans. Signal Process.*, vol. 8, no. 5, pp. 966–981, 2014.